

# Synthesis, characterization and photocatalytic activity of Titania nanotube

Renuka N. K.\* and Nikhila M.P.

Department of Chemistry, University of Calicut, Kerala – 673 635, India

\*Corresponding author: E-Mail: [nkrenu@gmail.com](mailto:nkrenu@gmail.com), Tel: 9447647790, Fax: (+91) 494 2400269

## ABSTRACT

Nowadays, extensive research has been undergoing in the fabrication of functional materials in nano regime having ordinary compositions. Various nanostructures of titania have been synthesized in this direction because of the higher efficiency of these systems towards a spectrum of applications such as photocatalysis, dye sensitized solar cells, sensors, drug delivery etc. In this paper Titania nanotube is synthesized by Hydrothermal method and is characterized by XRD, UVDRS, SEM, TEM, FTIR and surface area analysis. Photocatalytic efficiency of the prepared nanostructure was envisaged by conducting UV light induced photodegradation of Methylene blue (MB) dye. Titania nanotube showed superior activity towards the dye degradation when compared to the reference system prepared signifying the prepared nanostructure has commendable activity towards waste water treatment.

**KEY WORDS:** nanostructures, nanotube, hydrothermal method.

## 1. INTRODUCTION

Among the various semiconductor photocatalysts  $\text{TiO}_2$  has been considered as a promising one because of its chemical stability, nontoxicity, long durability strong oxidizing abilities (Nosaka, 2004; 2005; Janczyk, 2006) for the decomposition of organic pollutants (Fujishima, 2006; 2007), super hydrophilicity (Wang, 2006) and low cost. Factors such as size, specific surface area, crystalline phase, pore volume, pore structure, exposed surface facets may affects the photocatalytic performance of Titania significantly. Of the three polymorphic forms Anatase phase of  $\text{TiO}_2$  is found to be more active than the others namely rutile and brookite. Several  $\text{TiO}_2$  nanostructural materials, such as spheres (Bai, 2010; Chen, 2011), nanorods (Cozzoli, 2003; Feng, 2005), fibers (An, 2008; Cheng, 2010), tubes (Liu, 2008; Mor, 2005; Aoyama, 2012; Bavykin, 2006), sheets (Arabatzis, 1998; Caruso, 1998) and interconnected architectures (Poudel, 2005; Costal, 2009), have been fabricated owing to their excellent physicochemical properties that are catalytic, electronic, magnetic, mechanical and optical in nature. Thus, the construction of  $\text{TiO}_2$  nano structures with interesting morphologies and properties for superior performance has attracted considerable attention. Among the various nanostructures, there is an engrossing interest in the synthesis of  $\text{TiO}_2$  based nanotubes as they have high specific surface area, ion changeable ability and photocatalytic activity. There are many methods for synthesizing  $\text{TiO}_2$  nanotubes, but those having the anatase crystals may exhibit highest photocatalytic activity. In this direction the hydrothermal method has been proved superior for the synthesis of  $\text{TiO}_2$  nanotubes. In this paper we have synthesized Titania nanotubes by hydrothermal method in view of their potential applications in the field of photocatalysis. A thorough characterization was also made for the prepared sample.

## 2. MATERIALS AND METHODS

**2.1. Reagents:** Titanium dioxide anatase (Sigma Aldrich), sodium hydroxide (Merck, 98% purity), Hydrochloric acid (Merck), were used in the experiment. The water used throughout the experiment was distilled.

**2.2. Characterization:** Wide angle Powder X-ray diffraction (XRD) pattern of the sample was recorded using Rigaku D/MAX- diffractometer using  $\text{CuK}_\alpha$  radiation, in the Scan range of  $2\theta$ , 20-80°. The morphology of the samples was investigated using Transmission electron microscopy, TEM (FEI TECNAI 30 G2, 300KV) and Scanning electron microscope, FE-SEM (JEOL Model JSM-7600F), SEM (JEOL, Model JSM-6390LV) equipped with an Energy Dispersive Spectrometer (EDX). Samples for TEM were prepared by dropping the products on a carbon-coated copper grid after ultrasonic dispersing in water.  $\text{N}_2$  adsorption study was conducted on a Micromeritics Gemini surface area analyser using static adsorption procedure of  $\text{N}_2$  at 77K. The specific surface area of the system was calculated using the BET equation for data in  $p/p_0$  range between 0.05-0.299. Jasco FTIR-4100 spectrometer was used for recording the FTIR spectra of catalyst samples using KBr disc method. The UV-Vis diffuse reflectance spectrum was obtained using Jasco V-550 spectrophotometer, using  $\text{BaSO}_4$  as reference.

### 2.3. Sample Preparation

**2.3.1. Synthesis of titania nanotubes:** Titania nanotubes were synthesized following a literature procedure. About 5 g of Commercial  $\text{TiO}_2$  powder was dispersed in 175 ml of NaOH (10 N) solution using mechanical

stirrer for 1 hour and the suspension was transferred into a Teflon-lined stainless steel autoclave and sealed. The autoclave was maintained at a temperature of 130°C for 48 h and then allowed to cool to room temperatures. The white precipitate obtained from the hydrothermal treatment was vacuum-filtered and washed with 0.1 N HCl and deionized water until the pH was around 7. The sample was then dried at 100°C overnight and calcined at 300°C to obtain the titania nanotubes denoted as T2.

**2.4. Photocatalytic activity study:** The photocatalytic activity of the prepared system was monitored by examining the degradation of methylene blue dye in presence of UV lamp 98W ( $\lambda = 380\text{nm}$ ) at room temperature in a Luzchem LZC 4X model photoreactor. Continuous stirring is maintained throughout the reaction. For comparison the activity of the prepared titania is also determined. Catalyst dosage is 0.25g/L. Required amount of the catalysts were added to 75 ml of  $2.325 \times 10^{-5}\text{M}$  solution of methylene blue dye. Prior to illumination, the solution is stirred for 30 minutes under dark in order to reach adsorption-desorption equilibrium. The aqueous slurry is placed in the centre of the reactor and exposed to UV radiation with continuous magnetic stirring. Certain amount of the sample is taken from the beaker and centrifuged to remove the catalyst particles allowed to settle and the decanted solution is analyzed for the methylene blue content by measuring the absorbance at 663nm. The photocatalytic degradation percentage is calculated using the equation: Degradation percentage =  $[(C_0 - C)/C_0] \times 100$ , Where ' $C_0$ ' is the initial concentration of the dye solution and ' $C$ ' is the concentration after a definite time ' $t$ '.

**3. RESULTS AND DISCUSSION**

**3.1. Electron Microscopy Studies (SEM and TEM):** Fig.1 shows a high-magnification SEM image of the prepared titania nanotube. In figure tube-like structures are noticed. Tubular bundles are seen in some region that may be due to the aggregated nanotubes. The tubes are appeared to be open at the ends. The diameter of these tubes ranges from 12-15 nm, and their length ranges from 100-200 nm. The TEM image of titania nanotube [Fig.1b] clearly shows that tubes are uniform and open-ended which is extremely beneficial for adsorption and photocatalysis. The nanotubes were approximately 100–200 nm long and the diameter of the tube ranges from 8-15 nm.

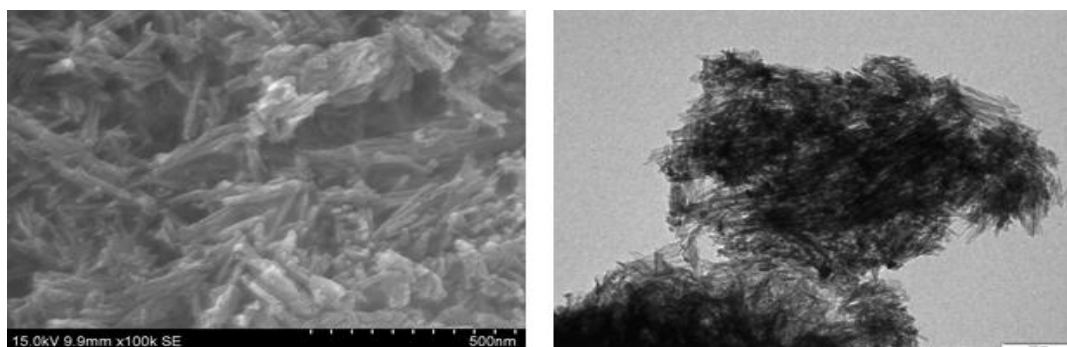


**Fig.1. SEM(a) and TEM(b) images of the prepared nanotube**

**3.2. XRD:** XRD pattern of titania nanotubes is represented in the figure as T2. From the diffraction pattern, characteristic diffraction peak at  $25.3^\circ$  for titania anatase (1 0 1) crystal face is observed. The characteristic peaks positioned at  $2\theta$  values 38.1, 48.0, 53.8, and 55.2 degrees are attributed to the diffractions of (004), (200), (105), (211), and (204) planes of anatase. The XRD pattern also indicated the presence of  $\text{H}_2\text{Ti}_3\text{O}_7$  by replacement of  $\text{Na}^+$  by  $\text{H}^+$  when the products were washed with water. The peak at  $2\theta$  value 10.130 represented the peak of hydrogen titanate phase ( $\text{H}_2\text{Ti}_3\text{O}_7$ ). The particle size was estimated by the Scherrer formula and was obtained as 31.3 nm.

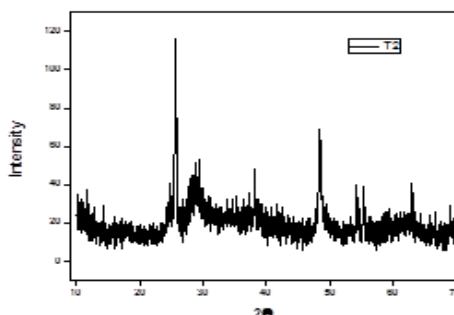


**Fig.2. XRD pattern of titania nanotube (T2)**

**3.3. FTIR Spectral data:** Fig.3 Shows typical FTIR spectrum of titania nanotube. The presence of crystallographic water molecules in the sample is confirmed by the appearance of a characteristic peak at 1631  $\text{cm}^{-1}$ , that can be assigned to the H–O–H deformation mode. The broad intense band at 3412  $\text{cm}^{-1}$  can be attributed to surface OH stretching mode oscillations. The broad band at 497.05 and 646.77  $\text{cm}^{-1}$  was assigned to Ti–O and Ti–O–Ti skeletal frequency region. The samples of titania nanotubes began to appear as a new peak at 1384  $\text{cm}^{-1}$ .

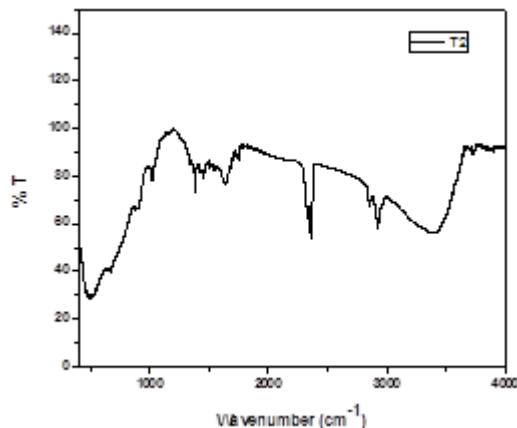


**Fig.3.FTIR spectrum of Titania nanotube(T2)**

**3.4. UltraViolet- visible Diffuse Reflectance Spectroscopy:** The UV-Vis absorption edge and band gap energies of the samples have been determined from the reflectance  $[F(R)]$  spectra using the KM (Kubelka–Munk) formalism and the Taucplot. For a semiconductor material, a plot of  $[F(R).hv]^n$  against  $h\nu$  should show a linear region just above the optical absorption edge for  $n=1/2$  if the band gap is a direct transition, or for  $n= 2$  if it is indirect[24-25]. Over the linear region of the plots, the relationship can be described as  $[F(R) hv]^{1/2}=K(h\nu-E_g)$  (1)

Where  $h\nu$  is the photon energy,  $E_g$  is the band gap energy, and  $K$  is a constant characteristic of the semiconductor material.

From Eq. (1) it appears that extrapolation of a Tauc plot to the X-axis should yield the band gap energy.

The band gap energy calculated from Kubolka-Munk plot (Fig. 4 a) was 3.25 eV. The band gap of the prepared titania nanoparticle is 3 eV. The titania nanotube showed higher band gap energies compared to the prepared titania (3eV) [Figure not shown.]. The high band gap Titania nanotube is attributed to the increase in the crystallite size of tube observed from XRD which in turn affects the band gap energies. A considerable blue shift is observed in the case of titania nanotube. The UV-visible absorption spectrum of Titania nanotube has been shown in the Fig.4b. The absorption spectrum showed a very broad band in the range 245- 295 nm.

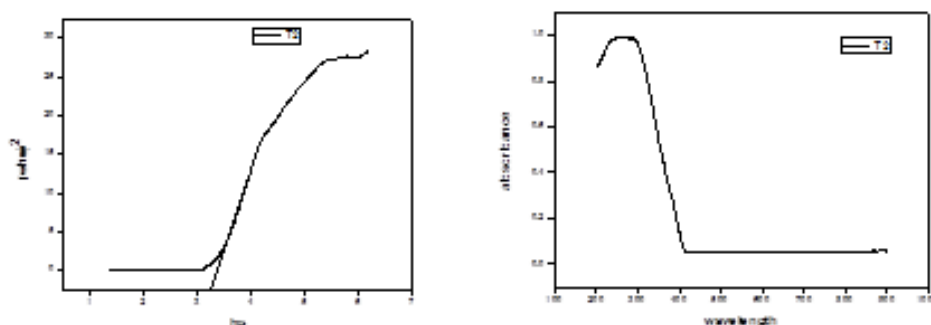


**Fig.4.Kubelka-Munk plot (a) and UVDRS spectrum(b) of Titania nanotube(T2)**

**3.5. Surface area:** Table 1 shows the BET surface areas of the nanotube and the prepared reference system titania. It can be seen that the titania nanotube is having higher surface area ( $S_{BET}$ , 84.79  $\text{m}^2/\text{g}$ ) which is of course new quality of the catalyst.

**Table.1.BET surface areas of the Samples**

Samples	$S_{BET}$
Titnia nanotube (T2)	84.79 $\text{m}^2/\text{g}$
Prepared titania(PT)	10.27 $\text{m}^2/\text{g}$

**3.6. Photocatalytic activity:** Photocatalytic activity of the prepared systems is analysed by measuring the extent of degradation of methylene blue dye in presence of UV light. For comparison, the photocatalytic activity of the prepared titania is also measured keeping the same experimental conditions. Degradation is carried out in the following conditions a) in the dark with catalysts b) in dark without catalyst c) in UV light without catalysts d) in UV light with catalysts. For the first three experimental conditions, Methylene Blue Concentration remains unchanged in the entire period under consideration for all the catalysts. A considerable degradation is observed only in the case of UV illumination in presence of catalysts. Figure 5 represents the UV-Visible absorption spectra for degradation of Methylene Blue Dye under UV light for the prepared nanostructures. A decrease in the absorption intensity is observed as the UV exposure time is increased. There is an increase in the degradation percentage with respect to irradiation time for all the systems [Fig.6 a]. A remarkable increase in the performance is observed for titania nanotubes when compared to the prepared titanium dioxide(PT). The percentage of degradation calculated at all time intervals is higher for the nanotube when compared to the Reference Titania prepared (PT). A sudden increase in the percentage of degradation is observed for nanotube during the first half of the reaction, which may be due to the high adsorption capacity of the system.

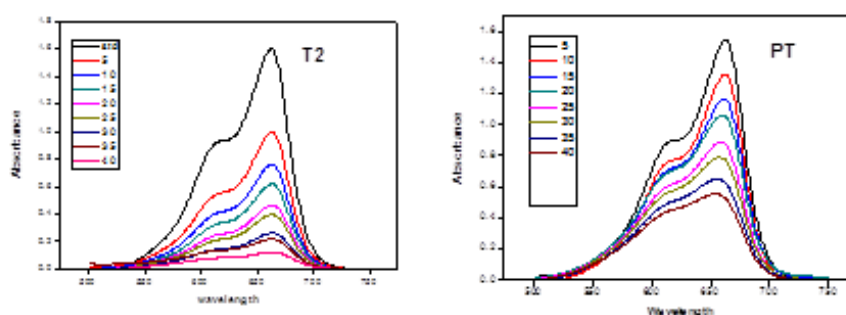


Fig.5 Time dependent UV-Vis Spectra of Titania nanotube (T2) and Prepared titania(PT)

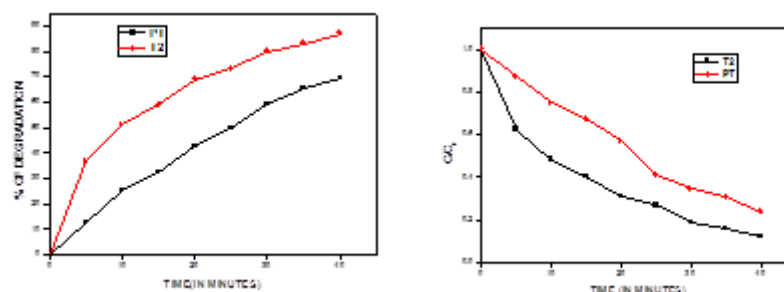


Fig.6 Photocatalytic degradation of the prepared Photocatalysts under UV Radiation(a); Photodegradation of Methylene Blue monitored as the normalized concentration change versus irradiation time(b)

Figure 6b represents the extent of degradation of Methylene Blue Dye over photocatalysts prepared. Photocatalytic reaction rates of the prepared systems were calculated from the pseudo first order rate equation,

$$\ln C_0/C = Kt$$

Where  $C_0$  is the initial concentration of the dye,  $C$  is the concentration after the time  $t$ .

Table.2. The rate constant obtained for various systems

Sample	Rate Constant( $\text{cm}^{-1}$ )
T2	0.04911
PT	0.03647

Titania nanotubes show higher activity than the reference titania, PT. The increased photocatalytic activity in UV light is attributed to the increased surface area and the observed blue shift in absorption of the prepared systems. The catalyst dosage taken is very low compared to those reported in literature. A significant enhancement in the surface area value than the previous reports by also highlights the quality of the catalyst.

**4. CONCLUSION**

Titania nanotube is prepared by hydrothermal method in order to control the microstructure, which enhances the photocatalytic activity. A reference system is also prepared and evaluated for the same. Synthesized samples were characterized by XRD, UVDRS, SEM, TEM, FTIR and BET Surface area analysis. Methylene Blue being a hazardous dye is photodegraded under UV light using the above mentioned photocatalysts. The performance towards the dye degradation followed the order, Titania nanotube > Reference titania prepared. Titania nanotube shows more activity in the UV light assisted photocatalytic degradation. The reason being the higher surface area along with the observed blue shift, when compared with the reference titania prepared.

**5. ACKNOWLEDGEMENT**

Nikhila M.P. would like to acknowledge University Grant Commission (UGC), for the junior research fellowship and University of Calicut for the research facilities.

**REFERENCES**

- Alexandre G.S.P, Leonardo L.C, Photocatalytic degradation of malachite green dye by application of TiO<sub>2</sub> nanotubes, *J. Hazard. Mater.*, 169, 2009, 297-301.
- An H, Zhu B, Li J, Zhou J, Wang S, Zhang S, Wu S, Huang W, Synthesis and characterization of thermally stable nanotubular TiO<sub>2</sub> and its Photocatalytic activity, *J. Phys. Chem. C.*, 112, 2008, 18772–18775.
- Aoyama Y, Oaki Y, Ise R, Imai H, Meso crystal nano sheet of rutile TiO<sub>2</sub> and its reaction selectivity as a photocatalyst, *Cryst. Eng. Comm.*, 14, 2012, 1405–1411.
- Arabatzi I.M, Falaras P, Synthesis of porous nanocrystalline TiO<sub>2</sub> foam, *Nano Lett.*, 3, 2003, 249–251.
- Bai H, Liu Z, Sun D.D, Hierarchically multifunctional TiO<sub>2</sub> nano-thorn membrane for water purification, *Chem. Commun.*, 46, 2010, 6542–6544.
- Bavykin D.V, Friedrich J. M, Walsh F. C, Protonated titanates and TiO<sub>2</sub> nanostructured materials: synthesis, properties, and applications, *Adv. Mater.*, 18, 2006, 2807–2824.
- Caruso R.A, Giersig M, Willig F, Antonietti M, Porous “Coral-like” TiO<sub>2</sub> structures produced by templating polymer gels, *Langmuir.*, 14, 1998, 6333–6336.
- Chen J.S, Chen C, Liu J, Xu R, Qiao S.Z, Lou X.W, Ellipsoidal hollow nanostructures assembled from anatase TiO<sub>2</sub> nanosheets as a magnetically separable photocatalyst, *Chem. Commun.*, 47, 2011, 2631–2633.
- Cheng Y, Huang W, Zhang Y, Zhu L, Liu Y, Fan X, Cao X, Preparation of TiO<sub>2</sub> hollow nanofibers by electrospinning combined with sol–gel process, *Cryst. Eng. Comm.*, 12, 2010, 2256–2260.
- Costa L, Prado A.G.S, TiO<sub>2</sub> nanotubes as recyclable catalyst for efficient photocatalytic degradation of indigo carmine dye, *J. Photochem. Photobiol. A*, 201, 2009, 45–49.
- Cozzoli P.D, Kornowski A, Weller H, Low-temperature synthesis of soluble and processable organic-capped anatase TiO<sub>2</sub> nanorods, *J. Am. Chem. Soc.*, 125, 2003, 14539–14548.
- Donga W, Sunb Y, Maa Q, Zhua L, Huac W, Lub X, Zhuanga G, Zhanga S, Guoa Z, Zhaoc D, Excellent Photocatalytic Degradation Activities of Ordered Mesoporous Anatase TiO<sub>2</sub>-SiO<sub>2</sub> Nanocomposites to Various Organic Contaminants, *J. Hazard. Mater.*, 229, 2012, 307.
- Feng X, Zhai J, Jiang L, The fabrication and switchable super hydrophobicity of TiO<sub>2</sub> nanorod films, *Angew. Chem. Int. Ed.*, 44, 2005, 5115–5118.
- Fujishima A, Zhang X, Titanium dioxide photocatalysis: present situation and future approaches, *C. R. Chim.*, 9, 2006, 750–760.
- Fujishima A, Zhang X, Tryk D.A, Heterogeneous photocatalysis: from water photolysis to applications in environmental cleanup, *Int. J. Hydrogen Energ.*, 32, 2007, 2664–2672.
- Huang H, Liu X, Huang J, Tubular Structured Hierarchical Mesoporous Titania Material Derived from Natural Cellulosic Substances and Application as Photocatalyst for Degradation of Methylene blue, *Mater. Res. Bull.*, 46, 2011, 1814.

Janczyk A, Krakowska E, Stochel G, Macyk W, Singlet oxygen photogeneration at surface modified titanium dioxide, *J. Am. Chem. Soc.*, 128, 2006, 15574–15575.

Liu Z, Zhang X, Nishimoto S, Murakami T, Fujishima A, Efficient photocatalytic degradation of gaseous acetaldehyde by highly ordered TiO<sub>2</sub> nanotube arrays, *Environ. Sci. Technol.*, 42, 2008, 8547–8551.

Mor G.K, Varghese O.K, Paulose M, Grimes C.A, Transparent highly ordered TiO<sub>2</sub> nanotube arrays via anodization of titanium thin films, *Adv. Funct. Mater.*, 15, 2005, 1291–1296.

Murphy A.B, Band-gap determination from diffuse reflectance measurement of semiconductor films, and application to photo electro chemical water-splitting, *Sol. Energ Mater. Sol C*, 91, 2007, 1326–1337.

Nosaka Y, Komori S, Yawata K, Hirakawa T, Nosaka A.Y, Photocatalytic [radical dot] OH radical formation in TiO<sub>2</sub> aqueous suspension studied by several detection methods, *Phys. Chem. Chem. Phys.*, 5, 2005, 4731–4735.

Nosaka Y, Daimon T, Nosaka A.Y, Murakami Y, Singlet oxygen formation in photocatalytic TiO<sub>2</sub> aqueous suspension, *Phys. Chem. Chem. Phys.*, 6, 2004, 2917–2918.

Poudel B, Wang W.Z, Dames C, Huang J.Y, Kunwar S, Wang D.Z, Banerjee D, Chen G, Ren Z.F, Formation of crystallized titania nanotubes and their transformation into nanowires, *Nanotechnol.*, 16, 2005, 1935–1940.

Seonghyuk Ko, Chandra K. Banerjee, Jagannathan Sankar, Photochemical synthesis and photocatalytic activity in simulated solar light of nanosized Ag doped TiO<sub>2</sub> nanoparticle composite, *Composites: Part B*, 42, 2011, 579–583.

Slamet H.W, Nasution E, Purnama, Kosela S, Gunlazuardi J, Photocatalytic reduction of CO<sub>2</sub> on copper-doped titania catalysts prepared by improved-impregnation method, *Catal. Commun.*, 6, 2005, 313–319.

Wang R, Hashimoto K, Fujishima A, Chikuni M, Kojima E, Kitamura A, Shimohigoshi M, Watanabe T, Light-induced amphiphilic surfaces, *Nature*, 388, 1997, 431–432.

Wang X, Li L, Lin Y, Zhu J, EDTA-Assisted Template-Free Synthesis and Improved Photocatalytic Activity of Homogeneous Znse hollow Microspheres, *Ceram. Int.*, 39, 2013, 213.

Yu X, Yu J, Cheng B, Huang B, One-Pot Template-Free Synthesis of Mono disperse Zinc Sulfide hollow Spheres and their Photocatalytic Properties, *Chem. Eur. J.*, 15, 2009, 6731–6739.